



## Characterization of sol–gel synthesised lead-free $(1-x)\text{Na}_{0.5}\text{Bi}_{0.5}\text{TiO}_3-x\text{BaTiO}_3$ -based ceramics

A. Chaouchi<sup>a,\*</sup>, S. Kennour<sup>a</sup>, S. d'Astorg<sup>b,c</sup>, M. Rguiti<sup>b,c</sup>, C. Courtois<sup>b,c</sup>, S. Marinel<sup>d</sup>, M. Aliouat<sup>a</sup>

<sup>a</sup> Laboratoire de Chimie Appliquée et Génie Chimique de l'Université Mouloud Mammeri de Tizi-Ouzou, Algeria

<sup>b</sup> Laboratoire des Matériaux Céramiques et Procédés Associés – Université de Valenciennes et du Hainaut-Cambrésis, Z.I. du Champ de l'Abbesse, 59600 Maubeuge, France

<sup>c</sup> Univ. Lille Nord de France, F-59000 Lille, France

<sup>d</sup> Laboratoire CRISMAT, UMR 6508 CNRS/ENSICAEN 6 Bd Maréchal Juin, 14050 Caen cedex, France

### ARTICLE INFO

#### Article history:

Received 21 March 2011

Received in revised form 17 June 2011

Accepted 17 June 2011

Available online 7 July 2011

#### Keywords:

$\text{Na}_{0.5}\text{Bi}_{0.5}\text{TiO}_3$

Lead-free ceramics

Sol–gel

Dielectrics

Ferroelectric

### ABSTRACT

The crystal structure, microstructure, dielectric and ferroelectric properties of  $(1-x)\text{Na}_{0.5}\text{Bi}_{0.5}\text{TiO}_3-x\text{BaTiO}_3$  ceramics with  $x=0, 0.03, 0.05, 0.07$  and  $0.1$  are investigated. A structural variation according to the system composition was investigated by X-ray diffraction (XRD) analyses. The results revealed that the synthesis temperature for pure perovskite phase powder prepared by the present sol–gel process is much lower ( $800^\circ\text{C}$ ), and a rhombohedral–tetragonal morphotropic phase boundary (MPB) is found for  $x=0.07$  composition which showing the highest remanent polarization value and the smallest coercive field. The optimum dielectric and piezoelectric properties were found with the  $0.93\text{Na}_{0.5}\text{Bi}_{0.5}\text{TiO}_3-0.07\text{BaTiO}_3$  composition. The piezoelectric constant  $d_{33}$  is  $120\text{ pC/N}$  and good polarization behaviour was observed with remanent polarization ( $P_r$ ) of  $12.18\text{ pC/cm}^2$ , coercive field ( $E_c$ ) of  $2.11\text{ kV/mm}$ , and enhanced dielectric properties  $\epsilon_r > 1500$  at room temperature. The  $0.93\text{Na}_{0.5}\text{Bi}_{0.5}\text{TiO}_3-0.07\text{BaTiO}_3$ -based ceramic is a promising lead-free piezoelectric candidate for applications in different devices.

© 2011 Elsevier B.V. All rights reserved.

### 1. Introduction

Sodium bismuth titanate  $\text{Na}_{0.5}\text{Bi}_{0.5}\text{TiO}_3$  (NBT) is of great interest as environmentally friendly alternatives to replace the widely used lead-based perovskite material [1–5].

The NBT ceramics is ferroelectric perovskite and has been discovered by Smolenskii et al. [6]. Two phase transformations, from the cubic phase to the tetragonal one and from the tetragonal to the rhombohedral one are observed in this system. The cubic–tetragonal phase transition corresponds to an electric order transformation from a paraelectric state to an anti-ferroelectric state, whereas the tetragonal–rhombohedral phase transition corresponds to a transformation from an anti-ferroelectric state to a ferroelectric one [7].

NBT is considered to be a promising candidate of lead-free piezoelectric ceramic because of its strong ferroelectricity with a large remanent polarization  $P_r$  of  $38\text{ }\mu\text{C/cm}^2$  [8]. However, NBT exhibits high coercive field,  $E_c$  of  $73\text{ kV/cm}$  and a relatively high conductivity making the poling process relatively difficult. Therefore, NBT-based ceramics that can be poled easier have recently been investigated

[9,10,12], and have been studied continuously by several research teams [10–14].

Among these research, Barium titanate,  $\text{BaTiO}_3$  (BT) and potassium bismuth titanate,  $\text{K}_{0.5}\text{Bi}_{0.5}\text{TiO}_3$  (KBT) are well-known lead-free piezoelectric materials with tetragonal phase. The binary systems of NBT–BT and NBT–KBT piezoelectric ceramics were reported by Takenaka et al. [15] and Sasaki et al. [16], respectively. Good piezoelectric and dielectric properties of these systems have been shown at compositions near the morphotropic phase boundary (MPB).

However, in their experimental work,  $(\text{Na}_{0.5}\text{Bi}_{0.5})_{0.94}\text{Ba}_{0.06}\text{TiO}_3$  powders were prepared by solid-state reaction via the calcination of  $\text{BaCO}_3$ ,  $\text{K}_2\text{CO}_3$ ,  $\text{Bi}_2\text{O}_3$  and  $\text{TiO}_2$  at high temperature of  $1000^\circ\text{C}$ . The resulting powders exhibit high agglomeration and heterogeneous particle size as a result of the high-temperature treatment. In comparison with other techniques, the sol–gel process has shown considerable advantages, including excellent chemical stoichiometry, compositional homogeneity, and lower crystallization temperature due to the mixing of liquid precursors on the molecular level [17–19]. With this point of view, in the present work the  $(1-x)\text{Na}_{0.5}\text{Bi}_{0.5}\text{TiO}_3-x\text{BaTiO}_3$  compositions were prepared by a sol–gel route. Structural, microstructural, electrical and piezoelectrical properties of these ceramics are presented.

\* Corresponding author.

E-mail address: [ahchaouchi@yahoo.fr](mailto:ahchaouchi@yahoo.fr) (A. Chaouchi).

## 2. Experimental procedures

The synthesis of the  $(1-x)\text{Na}_{0.5}\text{Bi}_{0.5}\text{TiO}_3-x\text{BaTiO}_3$  gel is based on the following steps. Titanium butoxide  $\text{Ti}(\text{OC}_4\text{H}_9)_4$  (99.5% pure) was diluted in absolute ethanol (99.5% pure) (solution 1). Bismuth nitrate pentahydrate  $(\text{Bi}(\text{NO}_3)_3 \cdot 5\text{H}_2\text{O})$  and barium acetate  $(\text{Ba}(\text{OOCCH}_3)_2)$  were dissolved in acetic acid (solution 2), and sodium nitrate  $(\text{NaNO}_3)$  was dissolved in distilled water (solution 3). The solutions 2 and 3 were stirred in order to make them homogeneous. Then, we added dropwise the mixture of solutions 2 and 3 to the solution 1, under stirring during 2 h. A homogeneous gel was obtained. This last was heated at  $110^\circ\text{C}$  overnight. Then the resulting dried gel was grounded with in an agate mortar to get the gel powder, and it was finally heat treated at various temperatures ( $500^\circ\text{C}$ ,  $600^\circ\text{C}$ ,  $800^\circ\text{C}$ ,  $900^\circ\text{C}$  and  $1000^\circ\text{C}$ ) for 2 h in air.

To manufacture pellets, an organic binder (Polyvinyl alcohol, 5 vol%) was manually added to the powder and disks (8 or 13 mm in diameter, 1.5 mm thick) were shaped by uni-axial pressing at a load of about 2100 kg. The green samples were finally sintered in air in a tubular furnace for 2 h at different temperatures, with heating and cooling rates of  $150^\circ\text{C}/\text{h}$ .

Thermogravimetry (TG) and DSC analysis of dried gel was carried out using a simultaneous thermal analyzer (Instruments NETZSCH STA 449F3) at a heating rate of  $5^\circ\text{C}/\text{min}$ . The density of the samples was measured by He-pycnometer (Accupyc 1330). The crystalline phase composition has been identified by X-ray diffraction (XRD) technique using the  $\text{Cu K}\alpha$  X-ray radiation (Philips X'Pert) and the microstructures were observed using a Scanning Electron Microscopy (SEM Philips XL'30).

The specimens were polished and electroded with silver paste. They were poled in a silicone oil bath under different poling conditions for piezoelectric measurements. The piezoelectric coefficient ( $d_{33}$ ) was measured using a piezoelectric  $d_{33}$  meter (Piezotest PM 200) at a frequency of 100 Hz. The dielectric properties were determined using HP4284A meter versus temperature (from  $20^\circ\text{C}$  to  $600^\circ\text{C}$ ). P-E hysteresis loops were obtained by Radiant Precision Workstation ferroelectric testing system.

## 3. Results and discussion

Fig. 1 shows the TGA/DSC curves carried out on dried gel of the sample in order to investigate phenomena occurring during the calcination process. The TGA/DSC curves (Fig. 1) revealed that the decomposition occurred in four different weight loss steps. The first main step, corresponding to 4.45% weight loss, is due to the vaporization of water and some organic compound at temperature between  $75^\circ\text{C}$  and  $200^\circ\text{C}$  as reported elsewhere [20], the DSC curve shows a large endothermic peak. The second step, corresponding to weight loss of 16.24%, was observed from  $200^\circ\text{C}$  to  $350^\circ\text{C}$ . This phenomenon is coupled to multi-exothermic peaks on DSC curve. It is related to the decomposition

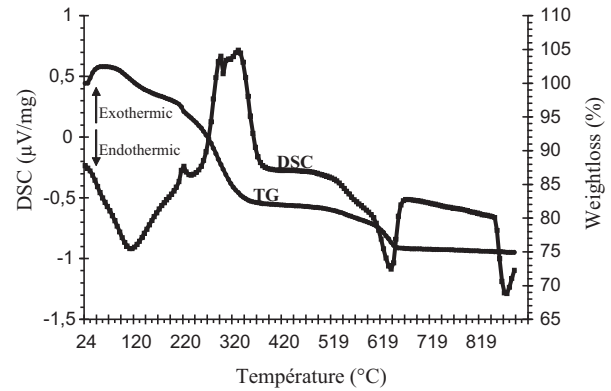


Fig. 1. Results of TG–DSC of the  $\text{Na}_{0.5}\text{Bi}_{0.5}\text{TiO}_3$  dried gel.

of some organic derivatives. The third step, corresponding to 5.18% weight loss at temperature between  $520^\circ\text{C}$  and  $650^\circ\text{C}$ , is probably due to the transformation of  $\text{Na}(\text{NO}_3)$ ,  $\text{Bi}(\text{NO}_3)_3$  and Ti-complex from disordered state to ordered state, and a small amount of  $\text{Na}_{0.5}\text{Bi}_{0.5}\text{TiO}_3$  was produced. At this step, the DSC curve shows an endothermic peak when temperature increased to above  $650^\circ\text{C}$ , showing that it does not remain any organic substance in the powder.

XRD analysis was carried out to study the phase evolution of the dried gels during the calcination processes. Fig. 2 shows the XRD patterns of dried gels calcinated at  $500^\circ\text{C}$ ,  $600^\circ\text{C}$ ,  $800^\circ\text{C}$ , and  $900^\circ\text{C}$ , respectively. After the thermal treatment at  $500^\circ\text{C}$  for 2 h, the perovskite phase was not detected. However, by increasing the calcination temperature to  $600^\circ\text{C}$ , peaks corresponding to the perovskite phase ( $\text{Na}_{0.5}\text{Bi}_{0.5}\text{TiO}_3$ ) were observed with some secondary peaks. Further increase of the temperature to  $800^\circ\text{C}$ , was sufficient to get a single phased powder of NBT perovskite. The above results show that the synthesis temperature for pure NBT perovskite phase powder prepared by the investigated sol–gel process is much lower than the required one with the conventional solid-state technique [18].

Fig. 3(b) shows the XRD patterns of  $(1-x)\text{Na}_{0.5}\text{Bi}_{0.5}\text{TiO}_3-x\text{BaTiO}_3$  ceramics in the  $2\theta$  ranges of

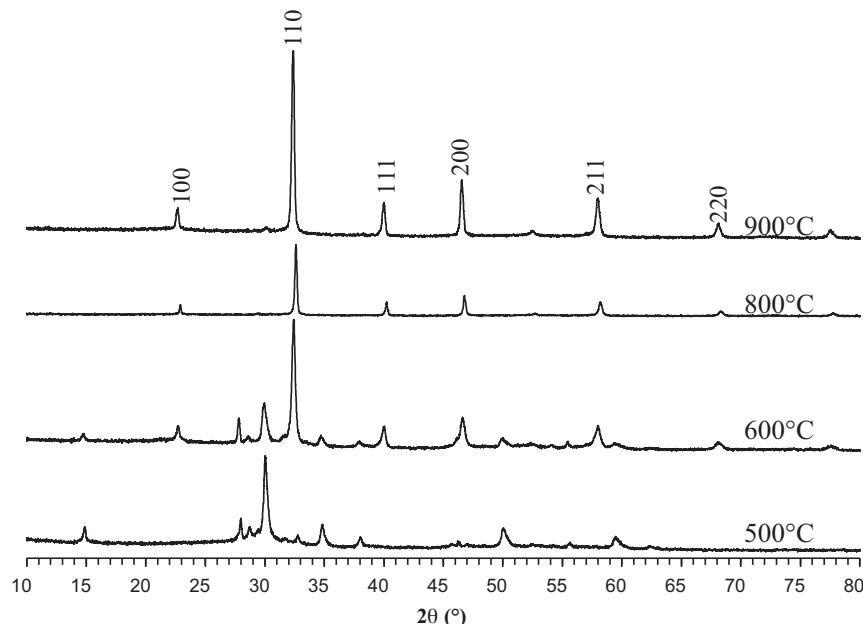
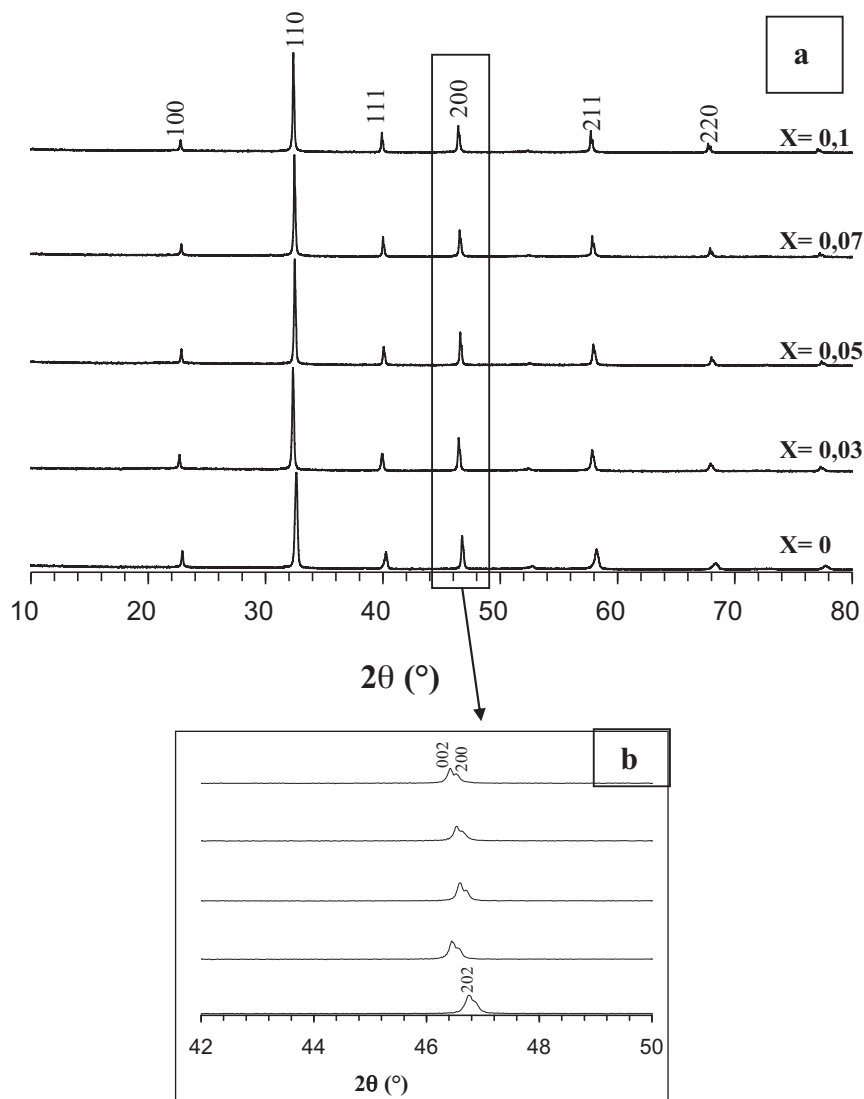


Fig. 2. X-ray diffraction patterns of the  $\text{Na}_{0.5}\text{Bi}_{0.5}\text{TiO}_3$  powders heat treated at different temperatures.



**Fig. 3.** (a): X-ray diffraction patterns of the  $(1-x)\text{Na}_{0.5}\text{Bi}_{0.5}\text{TiO}_3-x\text{BaTiO}_3$  ceramics sintered at  $1190^\circ\text{C}$  for 2 h. (b): (200) reflections in XRD patterns of  $(1-x)\text{Na}_{0.5}\text{Bi}_{0.5}\text{TiO}_3-x\text{BaTiO}_3$  ceramics.

$42\text{--}50^\circ$ . The rhombohedral symmetry for the system in the range of  $x=0\text{--}0.05$  is characterized by a (202) single peak between  $45^\circ$  and  $48^\circ$ . This peak splits to (002)/(200) peaks when  $x>0.05$ , corresponds to a tetragonal symmetry. Therefore, it can be suggested that the MPB of  $(1-x)\text{NBT-xBT}$  system ceramics lies in the composition range of  $0.06\leq x\leq 0.1$  at room temperature where rhombohedral and tetragonal phases coexist.

Fig. 4 shows scanning electron micrographs of sintered samples (polished and thermally etched). It is clearly observed that the grain size ranges from small to large grains, with clear grains boundaries and a random distribution within each sample. Pure NBT ceramic ( $x=0$ ) exhibits grains sizes from  $0.5$  to  $2\ \mu\text{m}$  and a quite large average grain size. By increasing  $x$ , it is shown that the final grains size decreases and that the distribution becomes more homogeneous. More particularly, with  $x=0.07$ , the average final grain size is about  $1\ \mu\text{m}$ .

The densification ratio of the samples ( $\rho(\%)=d_{\text{py}}/d_{\text{theo}}$ ), where  $d_{\text{py}}$  and  $d_{\text{theo}}$  are the experimental density and the theoretical one, respectively. The theoretical densities ( $d_{\text{theo}}$ ) for the

$(1-x)\text{Na}_{0.5}\text{Bi}_{0.5}\text{TiO}_3-x\text{BaTiO}_3$  ceramics were calculated using the following equation:

$$d_{\text{theo}} = \frac{(W_1 + W_2)}{(W_1/d_1) + (W_2/d_2)},$$

where  $W_1$  and  $W_2$ , are the weight ratio of  $(\text{Bi}_{0.5}\text{Na}_{0.5})\text{TiO}_3$  and  $\text{BaTiO}_3$ , respectively; and, where  $d_1$  and  $d_2$  are the densities of  $(\text{Bi}_{0.5}\text{Na}_{0.5})\text{TiO}_3$  ( $5.987\ \text{g/cm}^3$ ) and  $\text{BaTiO}_3$  ( $6.02\ \text{g/cm}^3$ ), respectively. The densification ratios  $\rho$  of the samples (sintered at  $1190^\circ\text{C}$  for 2 h) range from 95 to 98% of theoretical the one and are in good agreement with the scanning electron micrographs (Fig. 4). These ceramics obtained by a sol-gel route, exhibit larger densification ratio than the ceramics prepared by solid-state reaction [18].

Fig. 5 shows the temperature dependence of dielectric constant and dielectric losses of  $(1-x)\text{NBT-xBT}$  ceramics at 1 kHz. For different compositions, abnormal dielectric peaks have been observed and are attributed to phase transitions from ferroelectric to anti-ferroelectric (at  $T_d$ ) and from anti-ferroelectric to paraelectric (at  $T_m$ ), respectively. The maximum of permittivity ( $\epsilon_m$  at

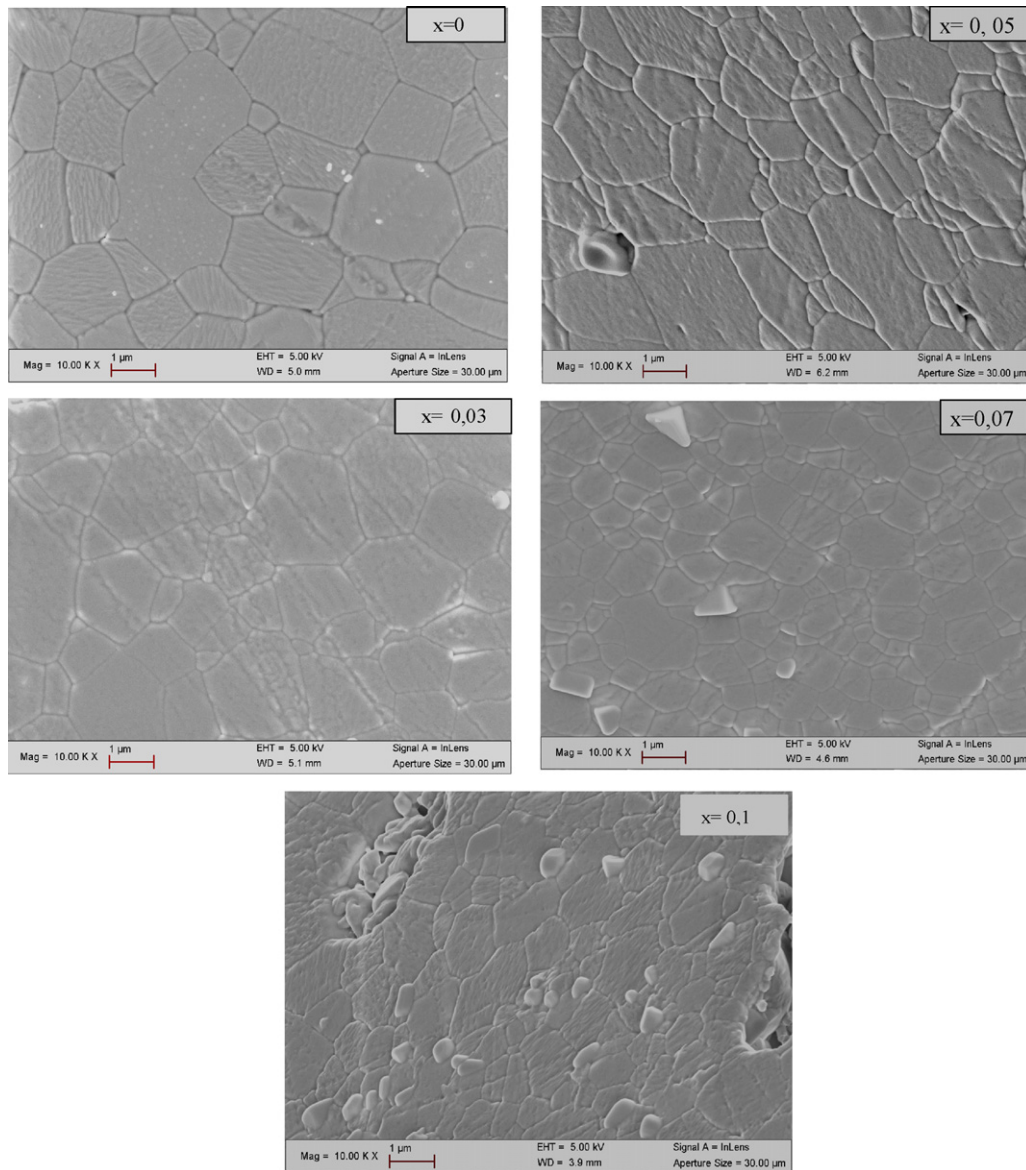


**Fig. 4.** Scanning electron micrographs of fracture for the  $(1-x)\text{Na}_{0.5}\text{Bi}_{0.5}\text{TiO}_3-x\text{BaTiO}_3$  ceramics sintered at  $1190^\circ\text{C}$  for 2 h.

$T_m$ ), the dielectric losses ( $\tan \delta$ ), and the  $T_d$  temperature depend on the BT content ( $x$ ). The maximal permittivity decreases by increasing  $x$  to 0.03 and 0.05. At  $x=0.07$  and 0.1, the ceramics exhibit higher dielectric constant than pure NBT ceramics ( $\varepsilon_m(x=0) = 2200$ , at 1 kHz). With  $x=0.07$ , the permittivity reaches a maximum  $\varepsilon_m = 4800$ . This higher value is due to the morphotropic phase boundary [21], and the highest material polarization [21]. The maximal temperature of dielectric constant ( $T_m$ ) decreases with increasing  $\text{BaTiO}_3$  content, from  $300^\circ\text{C}$  for  $x=0$  to  $250^\circ\text{C}$  for  $x=0.1$ .

Relatively low dielectric losses at room temperature are obtained for all samples (Fig. 5(b)), suggesting that the ceramics are well densified. It is shown that the losses  $\tan \delta$  slightly increase with temperature up to  $T_m$  and then increase drastically from  $T_m \approx 350\text{--}400^\circ\text{C}$ .

Fig. 6 shows the dielectric constant versus temperature of the NBT-0.07BT sample at 1 kHz, 10 kHz, 100 kHz respectively. This composition exhibits relaxor ferroelectric characteristics with broad peaks and frequency dependence: the higher the frequency,

the lower the dielectric constant, and the higher temperature  $T_m$ .

Fig. 7 shows the P-E loops of  $(1-x)\text{Na}_{0.5}\text{Bi}_{0.5}\text{TiO}_3-x\text{BaTiO}_3$  ceramics with  $x=0, 0.03, 0.05, 0.07$  and 0.1. As shown in Fig. 7(a), the P-E loops obtained at room temperature become slightly broadened,  $E_c$  and  $P_r$  increase slightly, as  $x$  increases from  $x=0$  to 0.07 and decreases for  $x=0.1$ . The P-E loop for  $x=0.07$  shows a good polarization behaviour, with coercive field  $E_c$  of  $2.8\text{ kV/mm}$  and remanent polarization  $P_r$  of  $12.18\ \mu\text{C cm}^{-2}$ .

Fig. 7(b) shows hysteresis loops obtained at  $70^\circ\text{C}$ . Heating the samples makes the polarization easier and it is shown that the P-E loop of the NBT-0.07BT ceramic is more rapidly saturated. The  $E_c$  coercive field is clearly decreased by performing the polarization process at  $70^\circ\text{C}$  ( $E_c = 1.7\text{ kV/mm}$ ), while  $P_r$  remains unchanged for  $x=0.07$ .

Fig. 8 shows the piezoelectric and dielectric properties of  $(1-x)\text{Na}_{0.5}\text{Bi}_{0.5}\text{TiO}_3-x\text{BaTiO}_3$  ceramics. The piezoelectric constant  $d_{33}$  and dielectric constant exhibit similar behaviours. The dielectric constant  $\varepsilon_r$  reaches a maximum value near the MPB

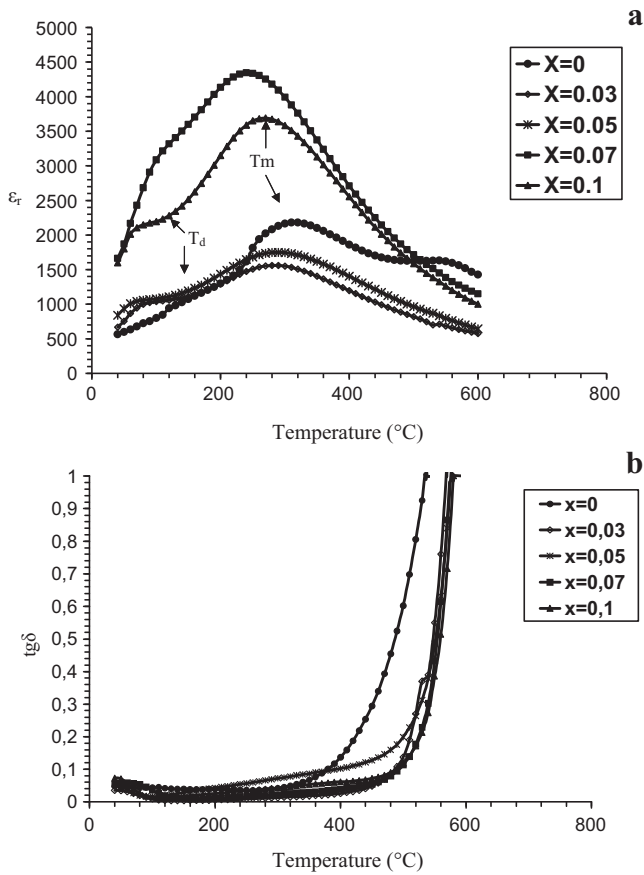


Fig. 5. Temperature dependence of permittivity and dielectric loss at 1 KHz of  $(1-x)\text{Na}_{0.5}\text{Bi}_{0.5}\text{TiO}_3-x\text{BaTiO}_3$  compositions.

( $x=0.07$ ). The piezoelectric constant  $d_{33}$  reaches a maximum value of  $120\text{ pC/N}$  at  $x=0.07$  and decreases drastically for  $x=0.1$  ( $d_{33}=64\text{ pC/N}$ ). Generally, high remanent polarization  $P_r$  and low coercive field  $E_c$  are presumably responsible for large piezoelectric properties. These properties show that the composition near the MPB exhibit large piezoelectric properties. It is attributed to an increase of possible spontaneous polarization directions for the composition near the MPB due to the coexistence of rhombohedral and tetragonal phases, eight polarization directions along  $(111)$  plan and six directions along  $(100)$  plan, respectively [22].

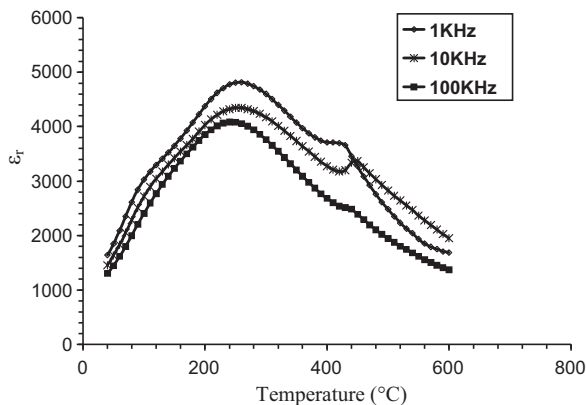


Fig. 6. Temperature and frequency dependence of dielectric constant of  $(1-x)\text{Na}_{0.5}\text{Bi}_{0.5}\text{TiO}_3-x\text{BaTiO}_3$  compositions.

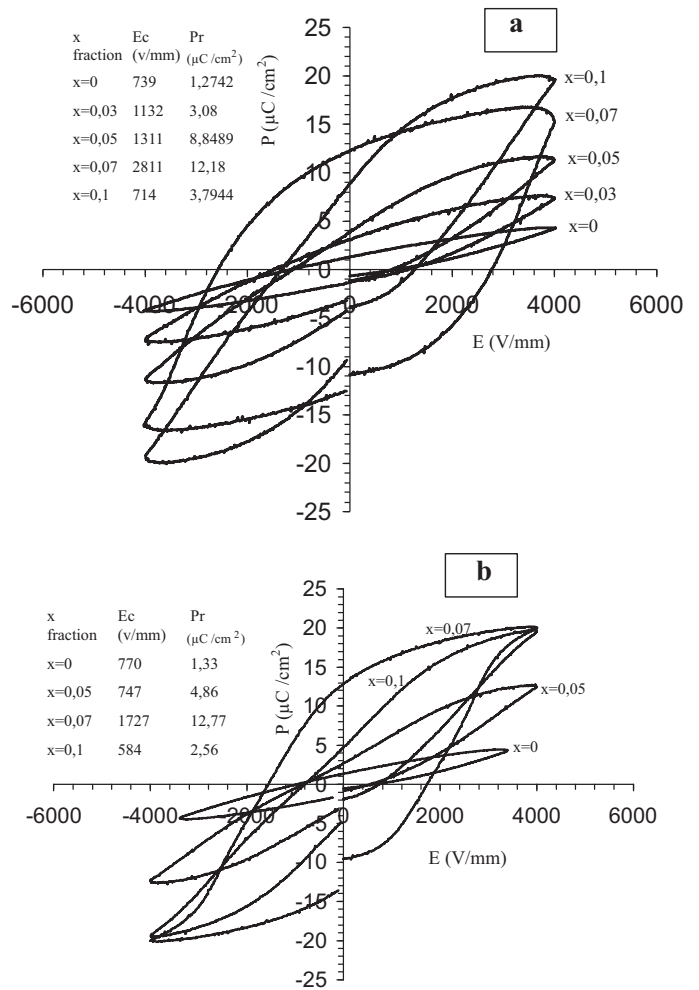


Fig. 7. P-E hysteresis loops of  $(1-x)\text{Na}_{0.5}\text{Bi}_{0.5}\text{TiO}_3-x\text{BaTiO}_3$  ceramics: (a) at room temperature, (b) at  $70^\circ\text{C}$ .

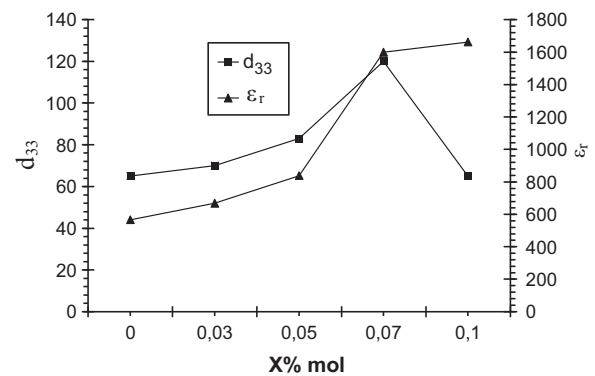


Fig. 8. Piezoelectric constant  $d_{33}$  and dielectric constant  $\epsilon_r$  of  $(1-x)\text{Na}_{0.5}\text{Bi}_{0.5}\text{TiO}_3-x\text{BaTiO}_3$  ceramics.

#### 4. Conclusions

$\text{BaTiO}_3$ -doped  $\text{Bi}_{0.5}\text{Na}_{0.5}\text{TiO}_3$  powders were synthesized by a sol-gel method using acetate, nitrates and alkoxide as reactants. Single phased perovskite powders were obtained with thermal treatment performed at  $800^\circ\text{C}$  for 2 h in air. Our results reveal that the  $0.93\text{Na}_{0.5}\text{Bi}_{0.5}\text{TiO}_3-0.07\text{BaTiO}_3$  ceramic exhibits good polarization behaviour, with interesting piezoelectric, dielectric and ferroelectric properties at room temperature ( $d_{33} = 120\text{ pC/N}$ ,

$\varepsilon_r = 1600$ ,  $\tan \delta < 0.05$ ,  $T_c = 250^\circ\text{C}$ . These results indicate that the ceramic is a promising candidate material for lead-free piezoelectric ceramics.

## References

- [1] Xiaolian Chao, Zupei Yang, Yunfei Chang, Mingyuan Dong, J. Alloys Compd. 477 (2009) 243.
- [2] Quan-Liang Zhao, De-Qing Zhang, J. Alloys Compd. 509 (2011) 6980.
- [3] P. Kumar, S. Singh, M. Spah, J.K. Juneja, C. Prakash, K.K. Raina, J. Alloys Compd. 489 (2010) 59.
- [4] S.K. Pandey, O.P. Thakur, D.K. Bhattacharya, Chandra Prakash, Ratnamala Chatterjee, J. Alloys Compd. 468 (2009) 356.
- [5] Zhonghua Yao, Hanxing Liu, Minghe Cao, Hua Hao, J. Alloys Compd. 505 (2010) 281.
- [6] G.A. Smolenskii, V.A. Isupv, A.I. Afranovskaya, N.N. Kainik, J. Solid State Phys. 11 (1961) 2651.
- [7] D.Z. Zhang, X.J. Zheng, X. Feng, T. Zhang, J. Sun, S.H. Dai, L.J. Gong, Y.Q. Gong, L. He, Z. Zhu, J. Huang, X. Xu, Alloys Compd. 504 (2010) 129.
- [8] Peng Fu, Zhijun Xu, Ruiqing Chu, Wei Li, Qian Xie, Yanjie Zhang, Qian Chen, J. Alloys Compd. 508 (2010) 546.
- [9] K.K. Sambasiva Rao, B. Tilak, K.Ch. Varada Rajulu, A. Swathi, Haileeyesus Workineh, J. Alloys Compd. 509 (2011) 7121.
- [10] Khairunisak Abdul Razak, Chiah Jun Yip, Srimala Sreekantan, J. Alloys Compd. 509 (2011) 2936.
- [11] Wei-Chih Lee, Chi-Yuen Huang, Liang-Kuo Tsao, Yu-Chun Wu, J. Alloys Compd. 492 (2010) 307.
- [12] S.E. Park, S.J. Chung, J. Am. Ceram. Soc. 79 (1996) 1290.
- [13] G.A. Smolenskii, V.A. Isupv, A.I. Afranovskaya, N.N. Krainik, J. Sov. Phys. Solid State 2 (1961) 2651.
- [14] XiaoMing Chen, XuXu Gong, TingNan Li, YuanHe, Peng Liu, J. Alloys Compd. 507 (2010) 535.
- [15] T. Takenaka, K.-I. Mareyama, K. Sakata, Jpn. J. Appl. Phys. 30 (1991) 2236.
- [16] A. Sasaki, T. Chiba, Y. Mamiya, Y. Mamiya, E. Otsuki, Jpn. J. Appl. Phys. 38 (1999) 5564.
- [17] Y.D. Hou, M.K. Zhu, L. Hou, J.B. Liu, J.L. Tang, H. Wang, H. Yan, J. Cryst. Growth 273 (2005) 500.
- [18] Y. Hiruma, R. Aoyagi, H. Nagata, T. Takenaka, Jpn. J. Appl. Phys. 43 (2004) 7556.
- [19] L. Hou, Y.D. Hou, M.K. Zhu, J.L. Tang, J.B. Liu, H. Wang, H. Yan, Mater. Lett. 59 (2005) 197.
- [20] R.A. Nyquist, R.O. Kagel, Infrared Spectra of Inorganic Compounds, Academic Press, New York, 1971.
- [21] T. Takenaka, K.I. Maruyama, K. Sakata, Jpn. J. Appl. Phys. Part 1 30 (1991) 2236.
- [22] C.A. Randall, N. kim, J.P. Kucera, W. Cao, T.R. Shrout, J. Am. Ceram. Soc. 81 (1998) 677.